5.5 AN AUTOMATED 2-D MULTI-PASS VELOCITY DEALIASING SCHEME

Jian Zhang[1] and Shunxin Wang[1]

[1] Cooperative Institute for Mesoscale Meteorological Studies, University of Oklahoma, Norman, OK, USA

1. INTRODUCTION

An operational challenge in using Doppler radar velocity field, whether for basic interpretation and/or as input into algorithms, is that velocity measurements are often aliased (folded). Aliasing occurs whenever the pulse repetition frequency (PRF) of the radar is lower than twice the Doppler frequency shift to be measured. Velocity measurements from Doppler weather radars are derived from the Doppler shifts (see Doviak and Zrnic, 1993 fro a detailed explanation). The maximum velocity that can be unambiguously measured is called the Nyquist velocity (or, "V_N" in this paper). Nyquist velocities of weather radars are usually 8 – 32 m/s. The radars can correctly measures velocities within the interval of ± V_N. Velocities outside the interval, however, cannot be correctly measured resulting in apparent values that reside within the interval of ± V_N. In general, the observed velocity values and their true values are related by:

$$V_T = V_O \pm 2n^* V_N \quad (1)$$

Here V_T represents the true velocity, V_O is the observed velocity, n is an integer (0, 1, 2,), and V_N represents the Nyquist velocity.

The correction of aliased velocities – the so-called dealiasing or unfolding – is a challenging technical task and becomes increasingly difficult with a decreasing Nyquist velocity. Since aliasing is easily identified as abrupt changes in the velocity data field, most of the dealiasing techniques are based on spatial and temporal continuities. These encompass spatial and temporal continuities from 1-dimensional (along a radial, e.g., Ray and Ziegler 1977; Bargen and Brown 1980), 2-dimensional (along both radial and azimuth, e.g., Merritt 1984; Boren et al. 1986; and Bergen and Albers 1988, Eilts and Smith 1990; Gong et al. 2003), to even 4-dimensional (along radial, azimuth, elevation, and time, e.g., James and Houze 2001). For the correction of aliased velocities, each velocity observation is compared with a reference velocity and the difference between the two is compared with a pre-specified wind-shear threshold. If the difference exceeds the threshold then the radial velocity in question is considered aliased and will be subject to correction until it is within the wind-shear threshold from the reference velocity.

Corresponding author address: Jian Zhang, NSSL, 1313 Halley Circle, Norman, OK 73069.
Email: jian.zhang@noaa.gov

Under most circumstances, the reference velocity is derived from the average of preceding neighbors of the velocity gate in question. The preceding neighbors are assumed to be correctly dealiased. However, at the boundaries, such as the first gates in each radial and first radial/gates in an isolated storm area, no preceding neighbors are available. In this case, independent velocity data, such as those from upper air soundings (e.g., Eilts and Smith 1990) and velocity azimuth display (VAD, e.g., Gong et al. 2003) are used. The upper air sounding data are usually very sparse in space (every 300+ km) and in time (every 12h). Hence, they are not representative of small-scale wind shears potentially leading to errors within velocity aliasing. The VAD winds are available more frequently in time and are spatially consistent with the velocity field to be dealiased. However, the VAD provides little information on horizontal variations in the wind field. In addition, VAD winds are subject to errors caused by the aliased velocities themselves (Gong et al. 2003). Errors in the reference velocity can propagate through the dealiasing process and sometime can fail the dealiasing for a whole sector. Therefore various error-proof measures have been implemented in the aforementioned techniques with varying success. The relatively simple and computationally efficient techniques (e.g., Eilts and Smith 1990) still have difficulties for cases with strong shear and small Nyquist velocities and in cases with large data voids. More elaborate error checking schemes (e.g., James and Houze 2001) while more robust result in long latency (for using a complete volume scan) and low computational efficiency (for temporal check) makes them less feasible for operational applications.

This paper presents a new multiple pass, 2D (radial and azimuth) technique and subsequent algorithm to obtain more accurate and reliable reference velocities from radar velocity observations. The new technique eliminates the dependency on external data sources while facilitating a dealiasing algorithm with a high computational efficiency for operational implementation. . Similar to Eilts and Smith (1990), the new technique is based on continuities in velocity fields along radial and azimuth directions. Multiple passes of dealiasing and error checking similar to the concepts in James and Houze (2001) are performed for robust dealiasing. The new multi-pass velocity dealiasing algorithm first finds a set of reference radials and gates by detecting the weakest wind region. Then from these reference radials and gates, the scheme checks continuities among

adjacent gates in radial and azimuth directions and corrects for the velocity values with large differences that exceed the pre-specified wind-shear threshold(s). Problematic velocity gates that do not have good reference velocities during an initial pass are not processed until a subsequent pass when additional good gates are identified.

The next section, section 2, describes each step in the new dealiasing algorithm. Case studies utilizing the dealiasing algorithm are presented in section 3 followed by a brief summary in section 4.

2. ALGORITHM DESCRIPTIONS

The new velocity dealiasing algorithm includes the following modules:

1) The initial radial searching;
2) The initial three reference radials dealiasing;
3) 1st round radial-by-radial dealiasing; and
4) 2nd round radial-by-radial dealiasing and error check.

Figure 1 provides an overview flowchart of the algorithm. Detailed descriptions for each individual module are provided in the following subsections.

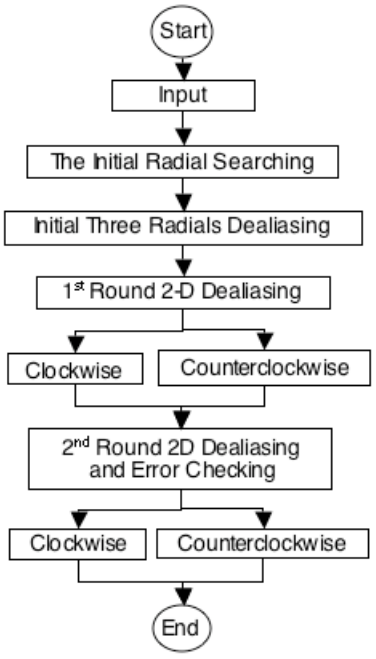

Fig. 1 An overview flowchart of the automated 2-D multi-pass velocity dealiasing algorithm.

2.1 The Initial Radial Search

In the previous dealiasing approaches, the initial reference velocity is usually derived from external data sources such as an upper air sounding or VAD. The external wind data are sometimes not representative of local velocity distributions due to temporal and spatial scales of the observations as in the case of soundings. In the new technique, the initial reference velocity is obtained using the radar velocity observations themselves. The technique begins by traversing all radials within a given tilt and finds a set of 'good' (or less likely aliased) radials. A good radial is defined as having no large wind shears between any adjacent gate pairs in the radial, i.e.:

$$|V_i - V_{i-1}| < \alpha V_N \tag{2}$$

Here i= 1, 2, …, N_0, represents all non-missing velocity gates; and α is an adaptable parameter with a default value of 0.8.

Within each of the 'good' radials, a conditional radial-wide mean velocity is calculated:

$$V_{M1} = \frac{1}{N_1}\sum_i V_i ; \qquad \text{where } |V_i| < \beta V_N \tag{3}$$

Here N_1 is the number of gates with velocity values that lie between $\pm ß V_N$ interval. ß is another adaptable parameter (default=0.3) for defining small velocity values.

If V_{M1} changes sign from two consecutive radials to the next two consecutive radials (Fig.2), then one of the two middle radials that has a larger N_1 is selected as the Initial Radial.

If an Initial Radial could not be found through the above approach, a second, iterative, search is carried out. In the second search, satisfying the following three criteria identifies a "good" radial:

1) no large wind shears between any adjacent gate pairs in the radial (see Eq. [2]);
2) have a large number of non-missing velocity gates, i.e., $N_0 \geq 40$; and
3) have a small mean of all the non-missing velocities, i.e., $V_{M0} = \frac{1}{N_0}\sum_i V_i$ and $V_{M0} < ß V_N$.

If more than one such "good" radials were identified, then the one with the smallest V_{M0} is selected as the Initial Radial. If no such radials were found in the first-pass search, then criterion 2) is relaxed by 5 (i.e., $N_0 \geq 35$) and another search for good radials is initiated. This process is repeated until an Initial Radial is identified or until N_0 becomes smaller than 5. If no good radial is found with $N_0 \geq 5$ and $V_{M0} < ß V_N$, then no dealiasing would be performed to the current tilt.

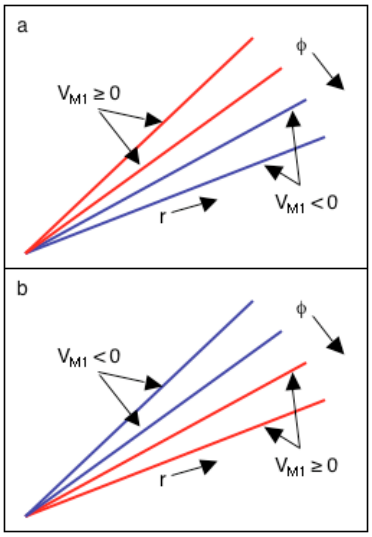

Fig. 2 An illustration of the initial approach for searching the Initial Radial. Here "r" indicates radial direction and "ϕ" indicates azimuth direction. The two panels illustrate two possible scenarios where V_{M1} changes sign from two consecutive radials to the next two consecutive radials. The Initial Radial is chosen as one of the two middle radials with a larger N_1.

Within each step of the new dealiasing algorithm, the data points are marked with five different flags to track processes that each point has gone through. The flag values range from 0 to 4 that represent: 0 -- unprocessed point; 1 -- processed point in the fist round and pre-first round; 2 -- processed point in the second round; 3 -- range folded point; and 4 -- missing value point. The flags serve as a confidence-level marker and different flags are handled differently during the dealiasing and error checking. Once a velocity gate is flagged as "1", it is considered a dealiased (i.e., "good") velocity and will not be processed further saving computational time and improving the overall algorithm efficiency.

2.2 Initial Three Reference Radials Dealiasing

This module first performs dealiasing for all points in the Initial Radial using V_{M1} (or V_{M0} depending on how the Initial Radial was identified) as the reference velocity. The module then processes the two neighbor radials of the Initial Radial through a two-steps dealiasing – first in azimuth direction and then in radial direction. In azimuth direction, the algorithm dealiases each velocity gate in the neighbor radials against the velocity at the same range in the Initial Radial. If a reference velocity is available in the Initial Radial, then the corresponding gate in the neighbor radial is processed and flagged as "1". Otherwise the gate in the neighbor radial is flagged as "0" ("unprocessed") and is postponed for later passes.

The radial direction dealiasing starts with a procedure of finding an Initial (good) Gate. The Initial Gate is defined as a dealiased velocity gate that encompasses:

1) at least 20 km (adaptable) contiguous non-missing neighbor gates on each side of the radial direction. This criterion is important to assure a reference velocity far away from echo boundaries.
2) at least 2 dealiased neighbor gates on each side along radial direction, which makes 5 contiguous good gates centered at the Initial Gate.
3) the 5 contiguous gates that satisfy Eq. (2).

Once the Initial Gate is found, the algorithm searches for the unprocessed gates along radial direction (both towards and away from the radar) starting from the Initial Gate. The unprocessed gates are dealiased using the average of three preceding good velocities in the same radial as a reference. The initial 5 contiguous good gates assure that a good reference gate can be found at least initially. If a break (e.g., missing-value or range-folded gate) is encountered during the searching/dealiasing, then a new search for another Initial Gate is performed. The searching/dealiasing are repeated until ends of the radial are reached. Any gates that get processed are marked with "1" and those do not are marked as "0" and left for subsequent processes. The radial direction dealiasing process is illustrated in Fig. 3.

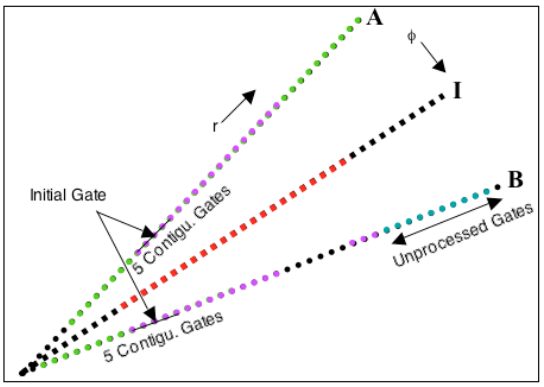

Fig. 3 An illustration of the initial three-reference radials dealiasing. The Initial Radial is marked with "I" and the two neighbor radials are marked as "A" and "B". The black points represent missing-values; the red points represent the gates that are processed in the Initial Radial. The purple gates are processed in the azimuth dealiasing using velocities (red dates) in the Initial Radial as references. The green gates are processed in the radial dealiasing process using the purple gates as references. The blue gates are not processed because a proper reference velocity is not found.

The Initial Radial and its two neighbor radials (total of three) will serve as reference data for the next step, the first round radial-by-radial dealiasing. Note that three instead of one initial radial are used in the current algorithm to avoid random errors propagating in the dealiasing process.

2.3 1st Round Radial-by-Radial Dealiasing

Starting from radials next to the three initial reference radials, the algorithm traverses through the tilt radial-by-radial in two passes: one in clockwise direction followed by one in counterclockwise direction. Each pass goes through 180 degrees (Fig. 4). The purpose of employing both clockwise and counterclockwise dealiasing is to improve the algorithm performance around shear zones. This strategy also restricts any potential error propagations inside a 180-degree sector.

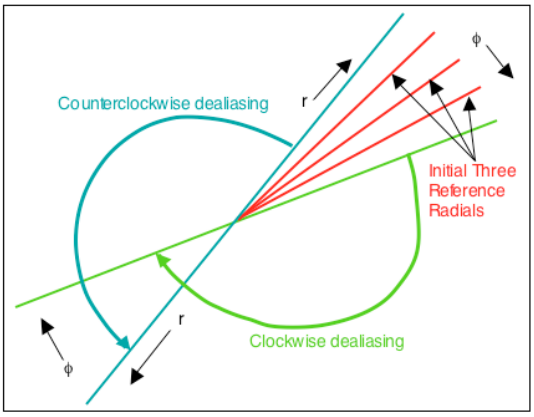

Fig. 4 Clockwise and counterclockwise radial-by-radial dealiasing using the initial three reference radials.

Each radial is processed in two-steps in the clockwise and counterclockwise passes: first in azimuth direction and then in radial direction. Along azimuth direction, each velocity gate is compare to a reference velocity, V_R, which is the average of three dealiased velocities in preceding radials (in clockwise direction or in counterclockwise direction) at the same range (Fig. 5). Three instead of one reference gate are used here to avoid incorrect dealiasing due to random errors in preceding velocity gates. The three good gates must satisfy the following criteria:

1) any two adjacent velocity pairs must satisfy Eq. (2); and
2) the difference between the current velocity, V, and V_R must be smaller than α*V_N.

If no 'good' V_R is found for any given gate, then the gate is flagged as "unprocessed" and postponed for subsequent dealiasing along the radial direction.

The dealiasing procedure along the radial direction is the same as in the initial three reference radials dealiasing except for the following criteria is used for Initial Gate identification (Fig. 5):

1) It must have at least 20 km contiguous non-missing neighbor gates on each side of the radial direction;
2) it must be a dealiased gate and must have at least 2 dealiased neighbor gates on each side along radial direction; which makes 5 contiguous good gates centered at the initial gate and the 5 gates must satisfy Eq. (2);
3) it must have at least 3 contiguous dealiased neighbor gates in preceding radials at the same range (Fig. 5); and the 3 velocities must satisfy Eq. (2).

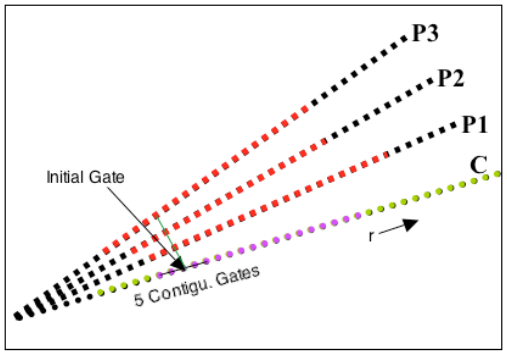

Fig. 5 Radial-by-radial dealiasing using the initial three reference radials. The red points indicate dealiased velocity gates in three preceding radials (P1, P2, and P3). The purple points indicate velocities in the current radial (marked as "C") that are dealiased using the average of the three preceding gates in azimuth direction; and green points indicate velocities that are dealiased along radial direction.

2.4 2nd Round Radial-by-Radial Dealiasing

The second round radial-by-radial dealiasing checks and performs dealiasing for all points that were not processed by the first round of radial-by-radial dealiasing. This module is similar to the first round but with a relaxed search radius for finding a reference velocity. For each unprocessed gate in the current radial (marked as "0", see Fig. 6), the algorithm first finds the three neighbor gates in preceding three radials (radials "-1", "-2", and "-3", Fig.6). If the three velocity gates satisfy the following conditions:

1) $|V_i - V_{i-1}| < \alpha V_N$, where i=-1 and -2; and
2) $|V_0 - V_R| < \alpha V_N$, where $V_R = \frac{1}{3}\sum_{i=-1}^{-3} V_i$,

then the V_0 gate is dealiased using V_R as reference. Otherwise, the searching goes one radial further back

and checks the three velocities at the same range as V_0 in radials "-2", "-3", and "-4". This procedure is repeated M times (M=3 as a default) or until a good V_R is found.

Along radial direction, the search for unprocessed gates starts at an arbitrary mid-range (e.g., 50 km) and proceeds both towards and away from the radar. The mid-range beginning is preferred over the first-gate beginning because random noises often exist near the radar due to residual clutter. Starting from the mid-range greatly reduces probabilities of error propagating in the dealiasing process. For any unprocessed gate, the algorithm searches for the nearest three contiguous dealiased gates along the radial direction both towards and away from the radar. The search is continued until three contiguous dealiased velocities are found or a range limit Δr (i.e., distance between the velocity gate in question and the closest gate in the three contiguous gates; default = 5 km) is exceeded.

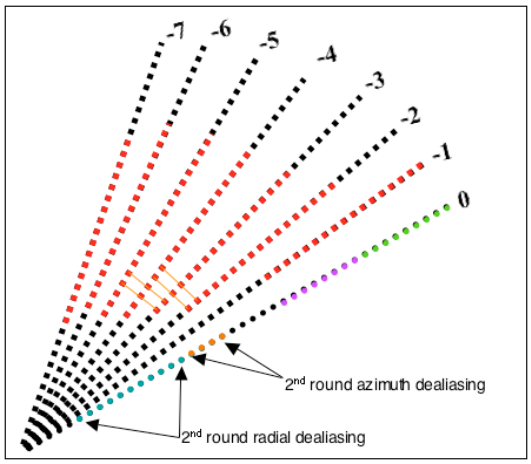

Fig. 6 An illustration of the 2nd round radial-by-radial dealiasing procedure. Radial "0" represents the current radial under processing. Radials "-1" to "-7" represent the preceding radials that have been processed and red points indicate "good" (dealiased) velocity gates. The purple and green points are "good" velocities that have been dealiased in the 1st round radial-by-radial dealiasing. The orange points represent the velocity gates that are dealiased using the three reference gates (marked by thin orange lines) found in azimuth direction within a relaxed searching radius. The blue points represent the velocity gates that are dealiased using three reference gates in radial direction.

The second round radial-by-radial dealiasing is repeated two more times with relaxed M (search radius in azimuth direction, default = 6 and 10 degrees, respectively, in the two additional passes) and Δr (search radius in radial direction, default = 20 and 50km, respectively, in the two additional passes). The additional two-passes are needed for dealiasing velocities in isolated storm regions away from the radar.

3. Case Studies

The new 2-D multi-pass velocity dealiasing algorithm has been tested for 6 days worth of data from WSR-88Ds located in Taiwan (RCWF) and in the United States (KTLX, Oklahoma; KMHX, North Carolinas). More than 1000 volume scans from events of F-5 tornadoes, Typhoons and Hurricanes were processed. The dealiasing algorithm performs very well in more than 99% of the aliased velocity observations (the aliased velocities were identified by human experts). There are less than 1% of the cases where the algorithm failed to recover the true velocities. They were primarily confined in small areas near range-folded velocity data. Below are examples of the dealiasing results for several different cases.

An independent velocity dealiasing scheme from the operational WSR-88D is also tested on the same data sets. Comparisons of results from the two schemes are shown below.

3.1 Continuous velocity fields

When the velocity field is continuous, both the new dealiasing algorithm and the operational WSR-88D algorithm are found to function very well. Figure 7 shows radial velocity fields before and after using the new dealiasing algorithm for the Typhoon Nari case as observed by RCWF (Wu-Fan-Shan, Taiwan) radar on 16 September 2001. The operational WSR-88D results (not shown here) are the same as the results from the new algorithm.

3.2 Aliased velocities near data voids

Figure 8 shows example dealiasing results from a case when aliased velocities are next to the Typhoon eye region. The new dealiasing scheme performed well for this case (Fig. 8b), so did the operational WSR-88D dealiasing algorithm (not shown).

3.3 Aliased velocities near data voids and near range folded areas

When significant data voids and discontinuities exist in the velocity field, dealiasing schemes often fail. Figure 9a shows an example velocity field observed during the Hurricane Isabel event on 18 September 2003. As a result of many range folded regions (purple hazes) and data voids, the operational WSR-88D dealiasing scheme incorrectly modified radial velocities in several areas (Fig. 9b). In contrast, the new 2-D multi-pass dealiasing algorithm was able to dealiase the velocity field correctly (Fig. 9c) except for a very small area to the west of the radar in the purple haze region at about 100 km of range. The accurate local reference

velocities that were identified through the iterative searching procedure helped to improve the dealiasing for this case. Furthermore, multiple error checks along both azimuth and radial directions helped minimizing any conflicts in the final velocity field.

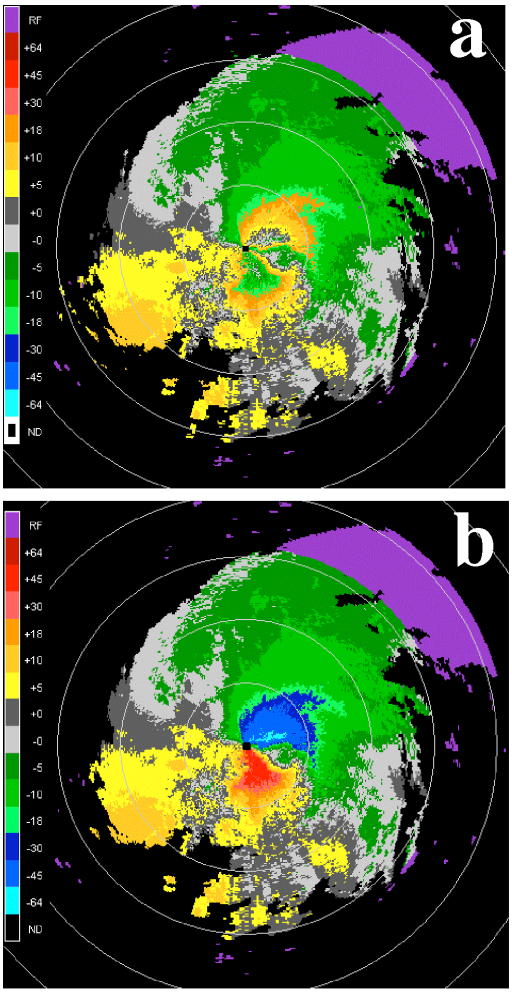

Fig. 7 Radial velocity fields before (a) and after (b) the dealiasing using the new algorithm. The data are from the RCWF (Wu-Fan-Shan, Taipei, Taiwan, Republic of China) radar valid at 1237UTC on 16 Sept. 2001. The range rings are 50 km apart.

3.4 Velocity fields with discontinuities

Figure 10 shows another example of a discontinuous velocity field. In this case, the operational WSR-88D dealiasing scheme failed to correct for the aliased velocity in the section south of the radar due to a discontinuity in the region (Figs. 10a and 10b). The new scheme successfully reconstructed the high 'negative' or inbound radial velocities in the region (Fig. 10c).

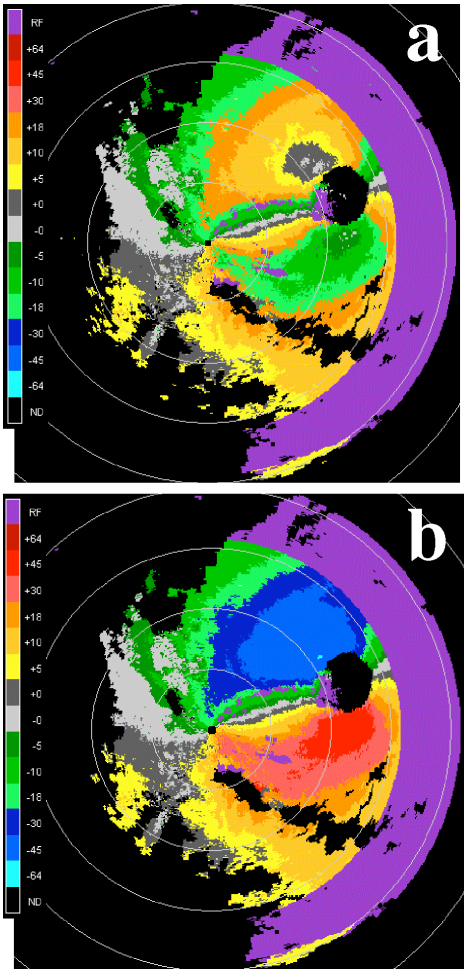

Fig. 8 Radial velocity fields before (a) and after (b) the dealiasing using the new algorithm. The data are from the RCWF (Wu-Fan-Shan, Taipei, Taiwan, Republic of China) radar valid at 0118UTC on 16 Sept. 2001.

4. Summary

A new 2-D multi-pass velocity dealiasing algorithm has been developed and tested. The algorithm is an automated scheme that finds reference velocities in the input velocity field. It is found that multi-pass neighborhood checking and iterative dealiasing procedures greatly improve the stability and robustness of the dealiasing algorithm. The algorithm can correct for aliased Doppler velocity data properly in more than 99% of the cases tested. The new algorithm is shown to be more robust than the current operational WSR-88D dealiasing scheme in regions near data voids and range folded observations. Future work will include background wind fields such as those from mesoscale models to further reduce uncertainties in reference velocities.

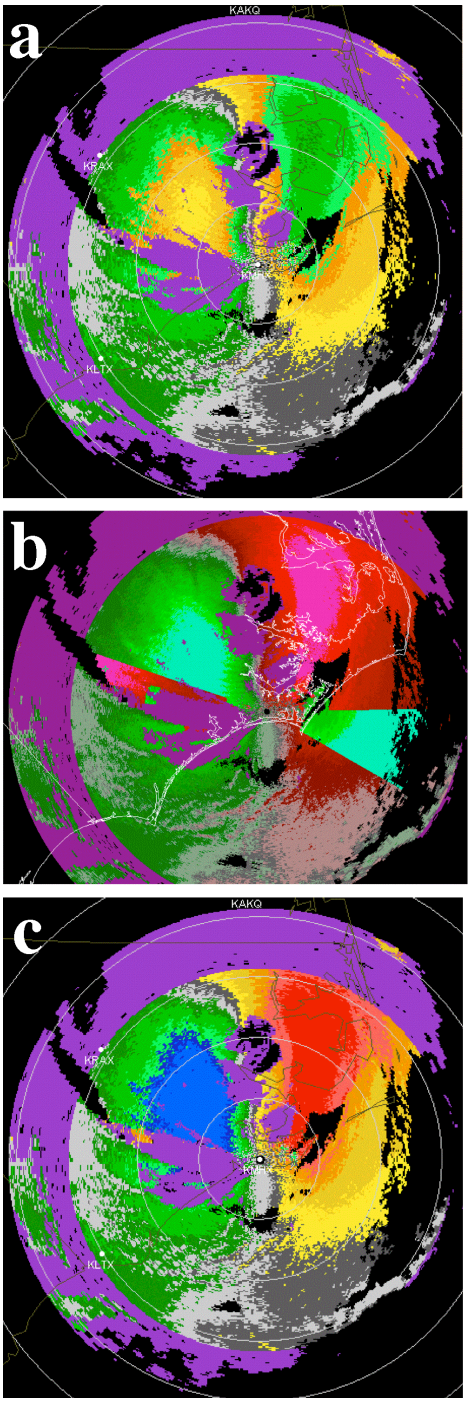

Fig. 9 Radial velocity field of 0.5 degree tilt observed by KMHX at 1959Z on 18 September 2003. Shown in the figure are a) raw velocity, b) dealiased velocity using the operational WSR-88D scheme, and c) dealiased velocity using the new algorithm.

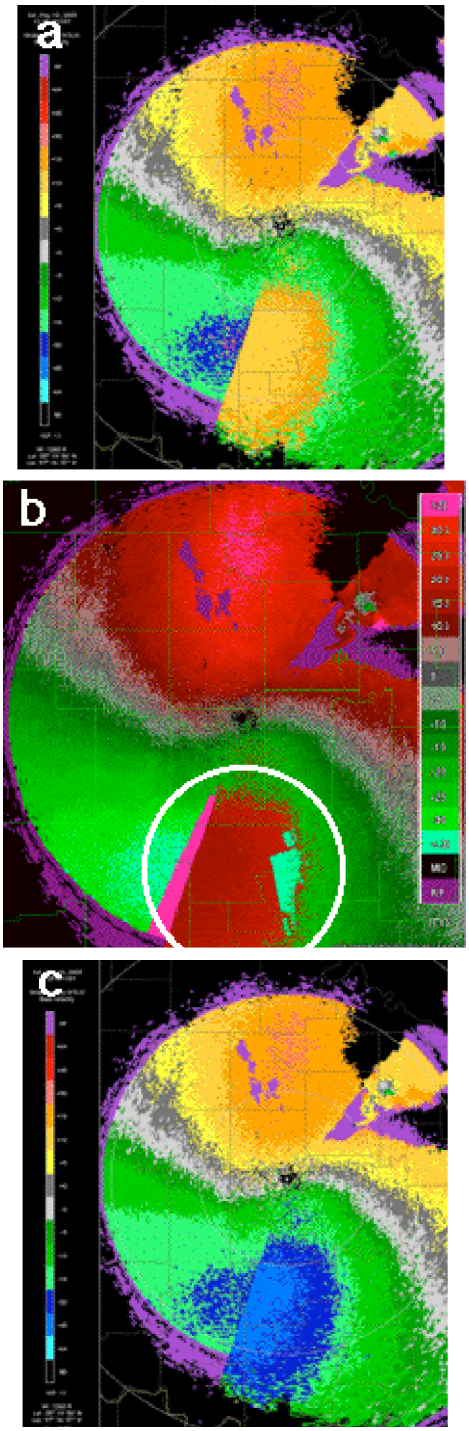

Fig. 10 Radial velocity field observed by KTLX on 0.5 degree tilt at 0523Z on 10 May 2003. Shown in the figure are a) raw, b) dealiased using the WSR-88D scheme, and c) dealiased using the new algorithm.

Acknowledgments

Major funding for this research was provided under the Aviation Weather Research Program NAPDT (NEXRAD Algorithms Product Development Team) MOU and partial funding was provided under NOAA-OU Cooperative Agreement #NA17RJ1227 and through the collaboration with the Central Weather Bureau of Taiwan, Republic of China.

This research is in response to requirements and funding by the Federal Aviation Administration (FAA). The views expressed are those of the authors and do not necessarily represent the official policy or position of the FAA.

References

Bargen, D.W., and R.C. Brown, 1980: Interactive radar velocity unfolding. *Proc. 19th Conf. On Radar Meteorology*, Miami, FL., Amer. Meteor. Soc., 278-283.

Bergen, W.R., and S.C. Albers, 1988: Two- and three-dimensional de-aliasing of Doppler radar velocities. *J. Atmos. Ocean. Tech.*, **5**, 305-319.

Boren, T.A., J.R. Cruz, and D.S. Zrnic, 1986: An artificial intelligence approach to Doppler weather radar velocity dealiasing. *Proc. 23rd Conf. On Radar Meteorology*, Snowmass, CO., Amer. Meteor. Soc., 107-110.

Doviak, R.D., and D.S. Zrnic, 1993: *Doppler Radar and Weather Observations*. 2nd Edition. Academic Press, 562pp.

Eilts, M.D., and S.D. Smith, 1990: Efficient dealiasing of Doppler velocities using local environment constraints. *J. Atmos. Ocean. Tech.*, **7**, 118-128.

Gong, J., L. Wang, and Q. Xu, 2003: A three-step dealiasing method for Doppler velocity data quality control. *J. Atmos. Ocean. Tech.*, **20**, 1738-1748.

James, C.N., and R.A. Houze Jr., 2001: A real-time four-dimensional Doppler dealiasing scheme. *J. Atmos. Ocean. Tech.*, **18**, 1674-1683.

Jing, Z., and G. Wiener, 1993: Two-dimensional dealiasing of Doppler velocities. *J. Atmos. Ocean. Tech.*, **10**, 798-808.

Merritt, M.W., 1984: Automatic velocity dealiasing for real-time applications. *Proc. 22nd Conf. On Radar Meteorology*, Zurich, Amer. Meteor. Soc., 528-533.

Ray, P. and C. Ziegler, 1977: Dealiasing first moment Doppler estimates. *J. Appl. Meteor.*, **16**, 563-564.